

PEGylated Liposomes as Carriers of Hydrophobic Porphyrins

Monika Dzieciuch,[†] Sami Rissanen,[‡] Natalia Szydłowska,[†] Alex Bunker,[§] Marta Kumorek,[†] Dorota Jamróz,[†] Ilpo Vattulainen,^{‡,||} Maria Nowakowska,[†] Tomasz Róg,^{*,‡} and Mariusz Kepczynski^{*,†}

[†]Faculty of Chemistry, Jagiellonian University, Krakow 31-007, Poland

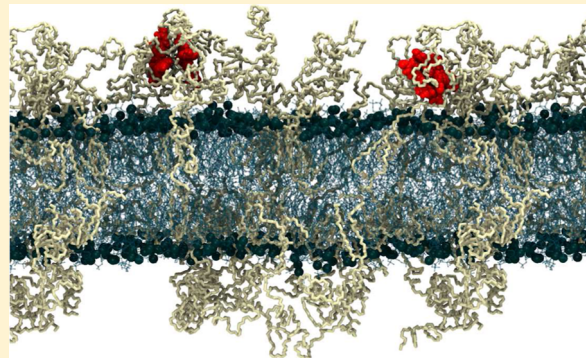
[‡]Department of Physics, Tampere University of Technology, Tampere 33720, Finland

[§]Centre for Drug Research, Faculty of Pharmacy, University of Helsinki, Helsinki 00100, Finland

^{||}MEMPHYS-Center for Biomembrane Physics, University of Southern Denmark, Odense 5230, Denmark

Supporting Information

ABSTRACT: Sterically stabilized liposomes (SSLs) (PEGylated liposomes) are applied as effective drug delivery vehicles. Understanding the interactions between hydrophobic compounds and PEGylated membranes is therefore important to determine the effectiveness of PEGylated liposomes for delivery of drugs or other bioactive substances. In this study, we have combined fluorescence quenching analysis (FQA) experiments and all-atom molecular dynamics (MD) simulations to study the effect of membrane PEGylation on the location and orientation of S₅,10,15,20-tetrakis(4-hydroxyphenyl)porphyrin (p-THPP) that has been used in our study as a model hydrophobic compound. First, we consider the properties of p-THPP in the presence of different fluid phosphatidylcholine bilayers that we use as model systems for protein-free cell membranes. Next, we studied the interaction between PEGylated membranes and p-THPP. Our MD simulation results indicated that the arrangement of p-THPP within zwitterionic membranes is dependent on their free volume, and p-THPP solubilized in PEGylated liposomes is localized in two preferred positions: deep within the membrane (close to the center of the bilayer) and in the outer PEG corona (p-THPP molecules being wrapped with the polymer chains). Fluorescence quenching methods confirmed the results of atomistic MD simulations and showed two populations of p-THPP molecules as in MD simulations. Our results provide both an explanation for the experimental observation that PEGylation improves the drug-loading efficiency of membranes and also a more detailed molecular-level description of the interactions between porphyrins and lipid membranes.



1. INTRODUCTION

Liposomes—approximately spherical enclosed structures formed from lipid bilayers—can be composed of a single type of amphiphilic lipid or be composed of several different lipid types, such as phospholipids or sterols. Their physical properties such as phase behavior, elasticity, and heterogeneity depend on lipid composition;¹ thus, the molecular composition of liposomes can be used to engineer their properties. The result is a tunable nanoscale pocket, with properties that can be designed to match those required by a given application. Quite often liposomes are used as carriers that protect and transport a contained payload. Liposomes have been used in this regard as drug carriers since the 1970s, resulting in a number of clinical applications, such as cancer chemotherapy and the treatment of fungal infections.² In addition, liposomes can be considered as simple models of biological membranes since they can be used, e.g., as tools to study passive uptake of drugs,³ a particular example being photosensitizers used in photodynamic therapy (PDT).⁴

While liposomes show considerable promise as drug carriers, they do have a significant weakness: once injected into the

bloodstream, they are vulnerable to attack from the reticuloendothelial system (RES). The first step of this process is a complex cascade of specific proteins binding to the surface of the xenobiotic (in this case a liposome), a process known as opsonization.⁵ Once a xenobiotic is opsonized, the resulting protein coating acts as a biochemical signal to macrophages in the liver and spleen,^{6,7} which in turn remove it from the bloodstream. As a result, liposomes have a bloodstream half-life of ~1 h. This half-life can be considerably extended through inclusion of lipids functionalized with a polymer to create a corona around the liposome, known as a “stealth sheath” which masks the liposome from RES. The current gold standard for polymers used in this fashion is poly(ethylene glycol) (PEG). When PEG is used to form the stealth sheath, the liposome is referred to as being “PEGylated”, often called a “sterically stabilized” liposome (SSL).⁸

Received: February 9, 2015

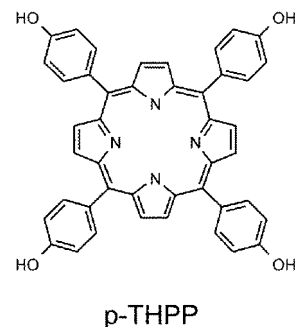
Revised: May 11, 2015

PEGylated liposomes are the most successful form of pharmaceutical nanocarrier to date, the most notable application being the first clinically approved nanocarrier based treatment, DOXIL.⁹ The mechanism through which PEGylation extends the bloodstream lifetime of drug delivery liposomes is not completely understood. It is however known to cause significant stabilization of liposome dispersions, prevent their aggregation, and inhibit protein and cellular interactions with liposomes. All of these effects are known to play a role in the protective effect of the PEG corona.⁶ The reason that PEG is such an effective polymer coating for pharmaceutical application is a result of its unique properties; it is nontoxic, soluble in both polar and nonpolar solvents,¹⁰ and can be eliminated from the body through a combination of renal and hepatic pathways.¹¹

An additional beneficial effect relates to partitioning of hydrophobic compounds into lipid membranes. The presence of the PEG corona around a liposome has been shown to have a significant effect on a property known as the *binding constant* (K_b) of these compounds to a lipid bilayer.¹ The binding constant indicates the affinity of a given compound to partition into a specified lipid membrane.⁴ For p-THPP, the value of K_b for phospholipid liposomes containing 7 mol % of PEG-lipid was found to be 2.6 times higher than the same characteristic for neat vesicles.¹ Thus, compared to non-PEGylated bilayers, porphyrin shows a considerably increased affinity for incorporation into PEGylated lipid membranes. PEGylation therefore results in a considerable increase in the loading efficiency of the liposomes for hydrophobic molecules.

PEGylation is known to alter the properties of phospholipid membranes.^{1,12–15} For instance, Yoshida et al.¹² investigated the effect of PEGylation on the liposome size, surface potential, microviscosity, micropolarity, and permeability of a 1,2-dipalmitoyl-*sn*-glycero-3-phosphocholine (DPPC) membrane and showed that the microviscosity and micropolarity of a liposomal bilayer have a maximum and a minimum value, respectively, at 6 mol % of PEG-lipid. The permeability of PEGylated liposomes was decreased in comparison to DPPC liposomes without PEGylation. We have previously demonstrated that a mixture of PEG-lipids added into liposomes reduces microviscosity in the hydrocarbon region of a membrane, while in the polar headgroup region fluidity is not affected.¹ Moreover, PEGylation resulted in a marked increase in the hydrophobicity of lipid membranes. For instance, when only 5 mol % of PEGylated lipids were added, the hydrophobicity reached a value similar to that of a phospholipid bilayer modified with 20 mol % of cholesterol. Tirosh et al.¹³ have demonstrated that intercalation of PEGylated lipids eliminates water from the lipid headgroup region of liposomes. In previous computational works, we performed several studies of the effect of PEGylation on phospholipid bilayers and found striking properties related to the interaction of PEG with the membrane interior, salt ions in the bloodstream, and targeting ligands.^{14–16}

The aim of this study was to explain the effect of liposome PEGylation on their drug-loading efficiency. p-THPP was applied as a model hydrophobic drug (the chemical structure of p-THPP is shown in Figure 1), since its partitioning properties to PEGylated and conventional liposomes have been evaluated experimentally.¹ Therefore, in this work we studied the embedding of the model porphyrin into both conventional and PEGylated liposomes using depth-sensitive fluorescence quenching analyses (FQA) and all-atom molecular dynamics



p-THPP

Figure 1. Chemical structure of p-THPP.

(MD) simulations. Computer simulations allow studies at atomistic resolution, revealing a level of detail that is often very difficult or even impossible to achieve experimentally.^{17–19} We used these MD simulations to determine the distribution of porphyrin molecules between the aqueous, lipid, and PEG regions of lipid membranes. Next, we focused on the depth-localization of p-THPP in lipid membranes and its orientation with respect to lipid molecules. To validate the results of MD simulations, we performed experimental measurements for the position of p-THPP inside a membrane using fluorescence techniques, especially FQA. The system studied in this paper can be treated as a model for the hydrophobic drug-PEGylated liposome interactions and the obtained results can be generalized for describing the behavior of other small organic molecules applied as drugs.

2. MATERIALS AND METHODS

2.1. Materials. 2-Oleoyl-1-palmitoyl-*sn*-glycero-3-phosphocholine (POPC, 99%) was purchased from Fluka. 5,10,15,20-Tetrakis(4-hydroxyphenyl)porphyrin (p-THPP, 95%) and stable free radicals (16-doxyloctadecanoic acid (16-SASL), 5-doxyloctadecanoic acid (5-SASL), and 3β-doxyloxycholestane (CSL)) were purchased from Aldrich. N-(Carbonylmethoxypoly(ethylene glycol) 2000)-1,2-distearoyl-*sn*-glycero-3-phosphoethanolamine and sodium salt (PEG₂₀₀₀-DSPE) was received from NOF Europe (Belgium) NV. All solvents were obtained from POCH (Gliwice, Poland) and were of spectroscopic grade. Millipore-quality water was used in the experiments.

2.2. Apparatus. Steady-state fluorescence spectra were recorded on an SLM-AMINCO 8100 Instruments spectrofluorometer at room temperature. Emission spectra were corrected for the wavelength dependence of the detector response by using an internal correction function provided by the manufacturer. Dynamic light scattering (DLS) measurements were performed using a Malvern Nano ZS light scattering apparatus (Malvern Instrument Ltd., Worcestershire, UK).

2.3. Preparation of Small Unilamellar Liposomes (SUV). POPC vesicles without quencher or containing one of the doxyl-spin labeled molecules (CSL, 5-SASL, or 16-SASL) were prepared by sonication as described previously.²⁰ Briefly, stock solutions of POPC and quenchers were prepared in CHCl₃. Appropriate volumes of the stock solutions were combined in a volumetric flask, and the solvent was evaporated under flow of nitrogen to complete dryness. The dry material was hydrated with a 10 mM phosphate buffer of pH 9 and vortexed for 2 min. The resulting multilamellar vesicle dispersion was subjected to five freeze–thaw cycles from liquid

Table 1. Summary of the Simulated Systems^a

system	p-THPP	lipid	DLPE-PEG	water	Na^+	Cl^-	simulation length (ns)
M1	4	128 POPC		4500			3×200
M2	4	128 DLPC		6700			500
M3	4	464 DLPC	48	60300	162	114	100
M4	2	464 DLPC	48	55100	48		350
M5	6	464 DLPC	48	44300	48		350
umbrella POPC	1	128 POPC		6700			45×200
umbrella DLPC	1	128 DLPC		7100			45×200
umbrella DLPE-PEG	2	464 DLPC	48	55139	48		200×100

^aThe table indicates the number of molecules/particles in the given system and the simulated time scale. In M1, the simulations for this system were repeated three times. “Umbrella” refers to umbrella simulations for the potential of mean force (see text for details).

nitrogen temperature to the temperature of 60 °C, followed by sonication at ice temperature for 10 min using a titanium tip SONICS VC 130. The final concentration of POPC was 2.5 mg/mL, and the lipid:quencher ratio was 80:20. The diameter of liposomes was in the range of 30–40 nm, as determined by DLS measurements. The vesicles were stored at 4 °C.

In the case of PEGylated liposomes, PEG₂₀₀₀-DSPE was dissolved in ethanol to form a stock solution. Next, appropriate volumes of stock solutions of POPC, PEG₂₀₀₀-DSPE, and one of the quenchers were mixed and the preparation of SUVs was continued as described above. The content of the PEGylated lipid was 7 mol %.

2.4. Fluorescence Quenching Measurements. The experiments were performed at pH 9 to avoid protonation of the quencher carboxyl group. It has been found earlier that the protonated form of the spin labels can change their position and move from one leaflet of the bilayer to the other.²¹ The appropriate volume of the SUV dispersion without quencher or comprising one of the quenchers was mixed with a solution of p-THPP in DMF. The samples were stirred for 20 h in the dark. The concentration of p-THPP was 0.88 μM, and the lipid:p-THPP ratio was ca. 3700:1. Fluorescence spectra of p-THPP incorporated into lipid membranes were recorded in a range of 620–770 nm using an excitation wavelength of 422 nm. At least six samples for each quencher were prepared. The presented results are averaged values.

Quenching with CuSO₄ was carried out using SUV dispersions with incorporated p-THPP ($c_{\text{p-THPP}} = 0.88 \mu\text{M}$). The increasing amount of a CuSO₄ stock solution (1 M) was added. After each addition of an aliquot, the solution was equilibrated for 10 min and the emission spectrum was measured.

2.5. MD Simulations. A summary of the studied systems is given in Table 1. We performed atomistic MD simulations for model systems containing: (1) Lipid bilayers composed of POPC (system M1) or 1,2-dilinoleoyl-sn-glycero-3-phosphocholine (2-18:2c9 PC (DLPC)) (system M2). The models included four p-THPP molecules placed at the interface (1 molecule) or inside a lipid membrane (3 molecules) (see Figures 2a,c). (2) DLPC bilayer with ~9 mol % of 1,2-dilinoleoyl-sn-glycero-3-phosphoethanolamine-N-[methoxy-(poly(ethylene glycol))-2000] (DLPE-PEG) and several p-THPP molecules placed at different initial positions. In system M3, four p-THPP molecules were initially located in bulk water (see Figure 3a). System M4 contained two p-THPP molecules: one located in bulk water and the other molecule immersed in the hydrophobic region of a PEGylated membrane (Figure 3c). In system M5, six p-THPP molecules were placed in the bilayer

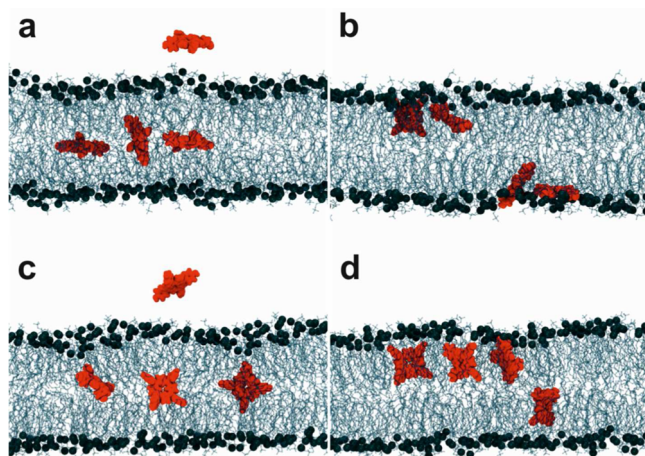


Figure 2. Images of the systems consisting of four p-THPP molecules in different membranes: in POPC (system M1) (a) at $t = 0$ and (b) after 200 ns of simulation and in DLPC (system M2) at (c) $t = 0$ and (d) after 200 ns. The porphyrin molecules are shown in red as a licorice representation. Lipid molecules are shown as blue sticks, with black spheres for phosphate groups. For clarity, water is not shown.

core (Figure 3e). The chemical structures of the compounds are shown in Figure S2.

In these studies we chose unsaturated lipids which are not typically used in drug delivery due to e.g. their susceptibility to oxidation. More typically in drug delivery studies one uses liposomes composed of saturated lipids and cholesterol. For example, the formulation of the very first FDA approved PEGylated liposome-based therapy DOXIL^{22,23} is composed of a mixture of DSPC, cholesterol, and DSPE-PEG. Thus, DSPC is clearly a relevant lipid to study in the context of PEGylation in liposome-based drug delivery. Unfortunately, diffusional and translational motions are very slow in this type of cholesterol-rich many-component system and would require substantially longer simulation times and are therefore not covered in this paper.

The free energy profile for the potential of mean force (PMF) was calculated for the p-THPP molecule by the umbrella sampling method,²⁴ using the GROMACS tool g_wham.²⁵ The PMF was obtained using 45 and 200 sampling windows in non-PEGylated and PEGylated bilayers, respectively, with distances of 0.1 nm between each window in the direction of membrane normal. The distances shown in the profiles are between the center of mass (COM) of the bilayer and the COM of p-THPP. Equilibration times of 100 and 20 ns were used in non-PEGylated and PEGylated bilayers, respectively, with respective production simulation times of

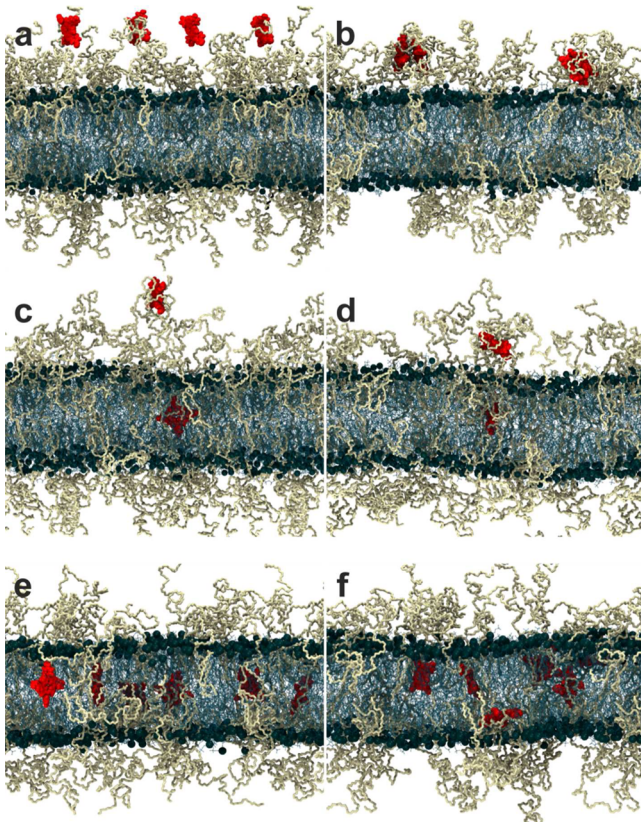


Figure 3. Images of the systems consisting of p-THPP molecules in DLPC/DLPE-PEG bilayers: four p-THPP molecules (system M3) at (a) $t = 0$ and (b) after 100 ns of simulation; two p-THPP molecules (system M4) at (c) $t = 0$ and (d) after 350 ns; and six p-THPP molecules (system M5) at (e) $t = 0$ and (f) after 350 ns. The porphyrin molecules are shown in red as a licorice representation. DLPC molecules are shown as blue sticks, with black spheres for phosphate groups. DLPE-PEG lipids are shown as beige sticks. For clarity, water and ions are not shown.

100 and 80 ns. To save computational resources, two p-THPP molecules were placed in each simulated system. The p-THPP molecules were located on opposite sides of a membrane separated by a distance of 6 nm to make sure that the p-THPP molecules were not able to interact with each other. The calculation of PMF is a tool we have previously used successfully to probe the properties in a wide range of biological systems.^{26–28}

All simulations were carried out using the GROMACS 4.5 software package.²⁹ To parametrize all lipid molecules, p-THPP, PEG, and ions, we used the all-atom OPLS force field.³⁰ Details of force field implementation and the choice of the partial charges can be found in our previous papers.^{14,31,32} For water, we used the TIP3P model that is compatible with the OPLS-AA force field.³³ The time step was set to 2 fs, and the simulations were carried out at 1 bar and 300 K. The v-rescale method³⁴ was used to couple the temperature with separate heat baths for the membrane and the rest of the system with time constants of 0.1 ps. The reference pressure set to 1 bar was maintained through the semi-isotropic Parrinello–Rahman barostat.³⁵ For long-range electrostatic interactions, we used the particle-mesh Ewald (PME) method.³⁶ The linear constraint solver (LINCS) algorithm was used to preserve covalent bond lengths.³⁷ Prior to all MD simulations, the

steepest-descent algorithm was used to minimize the energy of the initial configurations.

3. RESULTS

3.1. Fluorescence Quenching Studies. The vertical location of p-THPP in a lipid membrane was examined using nitroxide-labeled molecules (CSL, 5-SASL, and 16-SASL), which are known as efficient quenchers of fluorescence.²⁰ The chemical structures of the quenchers and approximate locations of the quenching moieties (nitroxide) across a phosphatidylcholine membrane are presented in Figure 4. The locations of

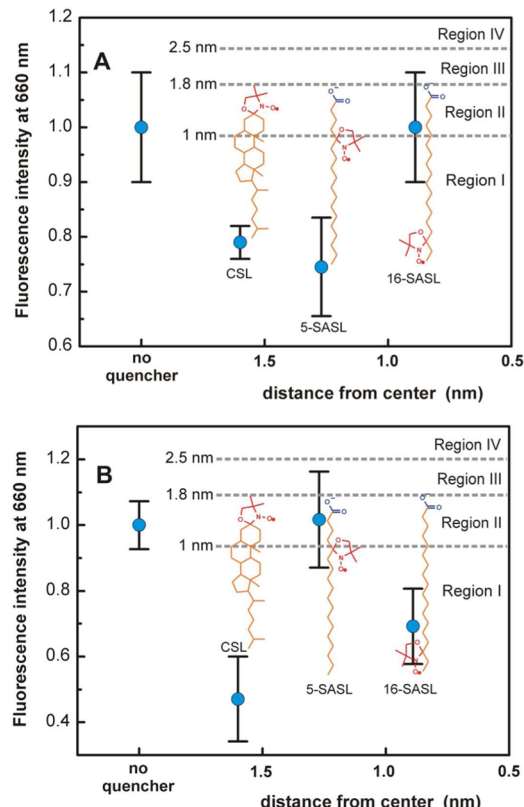


Figure 4. Quenching effect of nitroxide-labeled lipids (CSL, 5-SASL, and 16-SASL) on the fluorescence of p-THPP embedded into (A) pure POPC liposomes and (B) the PEGylated liposomes.

the quenching moieties of spin-labeled stearic acids were determined previously by MD simulations.²¹ The distance of the nitroxide group for 5-SASL and 16-SASL from the center of the bilayer was calculated to be 1.27 ± 0.22 and 0.86 ± 0.29 nm, respectively. Meanwhile, the position of CSL in a bilayer has not been examined previously. We thus assumed that the depth of the nitroxide group of CSL is similar to the depth of the cholesterol hydroxyl group. The vertical distance from the bilayer center to this group was hence estimated to be 1.6 nm.³⁸

We first prepared liposomes containing p-THPP and one of the quenchers. Then we measured the reduction of fluorescence intensity compared to that of the liposomes without quencher (Figure 4). The vertical localization of the fluorophore in a membrane can then be calculated by the parallax method,³⁹ where the basic idea is to compare the amount of fluorescence quenching caused by quenchers located in two different depths in a bilayer. Therefore, the distance of

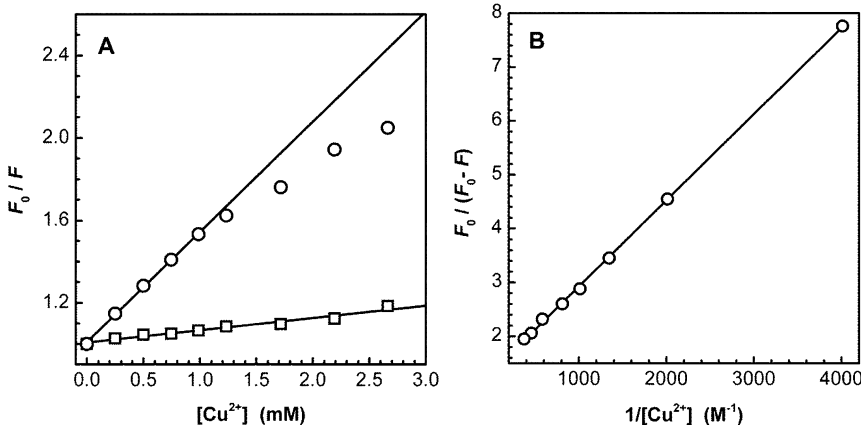


Figure 5. (A) Stern–Volmer plots for CuSO₄ quenching of p-THPP ($c_{p\text{-THPP}} = 0.88 \mu\text{M}$) in neat POPC (squares) and PEGylated (circles) membranes. (B) The modified Stern–Volmer plot for quenching of p-THPP in PEGylated membranes.

the fluorophore from the center of the bilayer (Z_{ef}) can be calculated as follows:

$$Z_{\text{ef}} = \frac{1}{2L_{21}} \left(\frac{1}{-\pi C} \ln \frac{F_1}{F_2} - L_{21}^2 \right) + L_{\text{cl}} \quad (1)$$

where F_1 and F_2 are the fluorescence intensities in the presence of the quencher that is located at a shallower or deeper position, respectively; L_{cl} is the distance from the bilayer center to the shallow quencher; L_{21} is the difference of the vertical locations of these two quenchers. C in turn is the concentration of the quencher in units of molecules per unit area at the bilayer surface.

As shown in Figure 4, the porphyrin group in the neat liposomes was mostly quenched by CSL and S-SASL. Thus, this pair of quenchers was chosen to determine the vertical position of p-THPP in the POPC membrane, Z_{ef} . Our calculations indicated that the center of the porphyrin ring is located at 1.36 nm from the bilayer center. For the case of the PEGylated liposomes, the largest quenching effect was observed for CSL and 16-SASL (Figure 4b). This finding clearly showed that p-THPP solubilized in the PEGylated liposomes was localized in two positions: deep in a membrane or closer to the membrane–water interface. The vertical position of the fluorophore molecules that were located deeper in a bilayer was calculated to be ca. 1.0 nm. The shallow position of p-THPP in the PEGylated membrane indicates that porphyrin tends to enter the PEG layer.

To confirm the results of the nitroxide quencher experiments, we performed quenching of the porphyrin fluorescence with copper ions. Cu²⁺ cations are not able to penetrate into the interior of lipid membranes.⁴⁰ Fluorescence quenching is associated with a quenching constant, K_{SV} , which is obtained from the Stern–Volmer equation:⁴¹

$$\frac{F_0}{F} = 1 + K_{\text{SV}}[Q] \quad (2)$$

where F_0 and F are the fluorescence intensities without and with the quencher, respectively; $[Q]$ is the quencher concentration.

To determine K_{SV} for p-THPP embedded in lipid membranes, we plotted the dependence of F_0/F versus $[Q]$ and fitted the data to eq 2. For the POPC liposomes, the Stern–Volmer plot was obtained for the whole concentration range and the value of K_{SV} was found to be $59.8 \pm 8.8 \text{ M}^{-1}$

(Figure 5A). Meanwhile, for PEGylated liposomes, a linear relation of F_0/F versus $[Q]$ was obtained up to the copper ion concentration of 1 mM, resulting in a value of $K_{\text{SV}} = 535 \pm 10 \text{ M}^{-1}$. For higher Cu²⁺ concentrations, the quenching of porphyrin fluorescence was characterized by a downward curving Stern–Volmer plot, indicating that a part of porphyrin molecules is prevented from making contact with the quencher. Quenching of the two fluorophore populations, one of which is inaccessible to the quencher, can be analyzed using a modified Stern–Volmer equation:⁴¹

$$\frac{F_0}{F_0 - F} = \frac{1}{f_a K_{\text{SV}}[Q]} + \frac{1}{f_a} \quad (3)$$

where K_{SV} is the Stern–Volmer quenching constant of the accessible fraction and f_a is the fraction of the initial fluorescence accessible to quencher. Fitting a line to a plot of $F_0/(F_0 - F)$ vs the reciprocal of the quencher concentration yielded f_a and K_{SV} to be 0.755 ± 0.025 and $828 \pm 56 \text{ M}^{-1}$, respectively (Figure 5B).

Porphyrin fluorescence was quenched by Cu²⁺ ions in both types of liposomes; however, the efficiency of this process was different for each lipid system. Cu²⁺ cations are not able to penetrate into the interior of lipid membranes but penetrate the water–membrane interface and interact with headgroups of PC membranes.⁴² The K_{SV} value for p-THPP in the POPC liposomes was much lower than that found for p-THPP embedded into the PEGylated liposomes. This suggested that p-THPP in POPC liposomes was located inside the bilayer, whereas in PEGylated liposomes it was positioned closer to the water phase. Moreover, in this case there were two populations of p-THPP. One population, accessible to the quencher, is probably due to the dye molecules embedded into the polymeric corona. The molecules that were buried in the bilayer, thus being unavailable to the quencher, likely constitute the other fraction.

3.2. Results Based on MD Simulations. **3.2.1. p-THPP in Non-PEGylated Membranes. Self-Assembly Process.** We first considered the location (depth) and arrangement of p-THPP molecules inside non-PEGylated lipid bilayers (Figure 2). Membranes composed of pure POPC or DLPC were used in the simulations. Figure S4 (see Supporting Information) depicts how the p-THPP molecules moved along the bilayer normal direction (z -coordinate). In these plots, the interfaces of the bilayer–water phases are shown as dashed horizontal black

lines, describing the average positions of the phosphate groups. Figures S4b, S4c, and S4d show that the porphyrin molecules initially located in the aqueous phase migrated into the POPC bilayer within 20–30 ns. For the DLPC membrane this assembly process took place much more slowly, in about 300 ns (Figure S4a). All subsequent analyses were carried out only for the data from the final part of the trajectory, when all the p-THPP molecules were immersed in the lipid bilayers. In none of the cases discussed above did we find translocation of p-THPP across a membrane. The barrier for translocation is therefore rather large, as was determined also from free energy calculations (see below).

Porphyrin Location. Selected snapshots taken at the end of the simulations, illustrating the location and orientation of porphyrin in the lipid bilayers, are shown in Figures 2b and 2d. They indicate that the preferred position and arrangement of p-THPP were different for the two types of bilayers.

To elucidate the position of porphyrin with respect to lipid molecules, we calculated their mass density profiles across a membrane. Figure 6a shows that porphyrin had two favorite

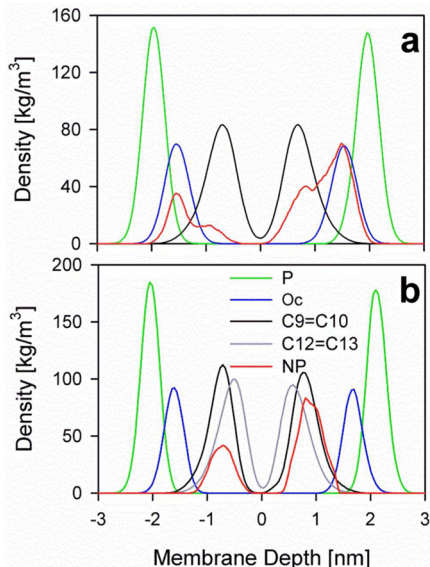


Figure 6. Mass density profiles of porphyrins and selected lipid atoms along the bilayer normal as averaged over the last 100 ns of the trajectories for (a) POPC and (b) DLPC membranes. The profiles are colored as follows: red lines (standing for porphyrin nitrogen; scaled 10 times), blue lines (carbonyl oxygens), green lines (phosphate groups), and black and gray lines (double bonds as shown in the inset). The asymmetry in the p-TPPH distributions results from the different number of p-TPPH molecules in the upper and lower leaflets.

locations in a POPC bilayer. The p-THPP profile has two maxima at ~0.90 and ~1.53 nm from the bilayer center and overlaps with the profiles of the carbonyl groups and the double bonds of lipids. In the DLPC membrane, the porphyrin profile has a maximum at ~0.85 nm and partly overlaps with the profiles of lipid double bonds. Thus, the presence of additional double bonds in the DLPC structure (see Figure S2) shifts the p-THPP location deeper into the membrane.

Subsequently, we calculated free energy profiles for p-THPP migrating from the aqueous phase to a lipid bilayer. The profiles were calculated for both POPC (system “umbrella POPC”) and DLPC (system “umbrella DLPC”) bilayers. The results are shown in Figure 7. For the case of the POPC bilayer,

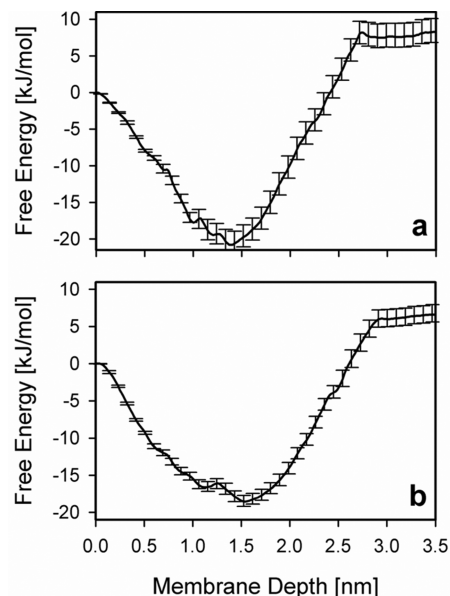


Figure 7. Free energy profiles of p-THPP along the membrane normal in the (a) DLPC and (b) POPC bilayers. Statistical errors were estimated using the bootstrap analysis.

two resolved minima located at ~1.1 and 1.6 nm from the bilayer center were clearly observed. These minima correspond to maxima in the density profile of p-THPP. For the DLPC bilayer, the deepest minimum in the free energy profile is located at a depth of 1.3 nm from the bilayer center. Two shallower minima located at a shorter distance from the bilayer center can also be observed. This indicates that the porphyrin position in the DLPC bilayer is more complex than the image resulting from the density profiles. We would like to point out that there are small discrepancies between the positions of the peaks in the free energy profiles and density plots. This is not actually a surprising result, since the calculation methodology of the density profiles and the free energy profiles are quite different. First of all, in free energy calculations an additional biased force is used, which can slightly modify system properties. Second, in the free energy calculations the position of the center of mass is shown, while the density profile shows the position of the central nitrogen atoms. They do not have to be exactly the same due to the too small mobility of the phenol rings.

Importantly, we observed through free energy calculations (Figure 7) that there is a high free energy barrier for p-THPP molecules to translocate from one leaflet of the membrane to the other. The translocation barrier is about 18.5 and 20.8 kJ/mol for the POPC and DLPC membranes, respectively. For comparison, the free energy barriers for translocation of p-THPP from a bilayer to the water phase are higher, being 25.8 and 29.8 kJ/mol for the POPC and DLPC bilayers, respectively.

Orientation of Porphyrin in a Membrane. To describe the orientation of the porphyrin ring inside a membrane, we used the angle θ_n between the bilayer normal and the normal of the p-THPP ring. Since the p-THPP molecules are characterized by two distinct locations in the POPC bilayer, we calculated the distribution of their orientation as a function of their position along the bilayer normal direction. Two-dimensional maps of the distribution of θ_n are shown in Figure 8.

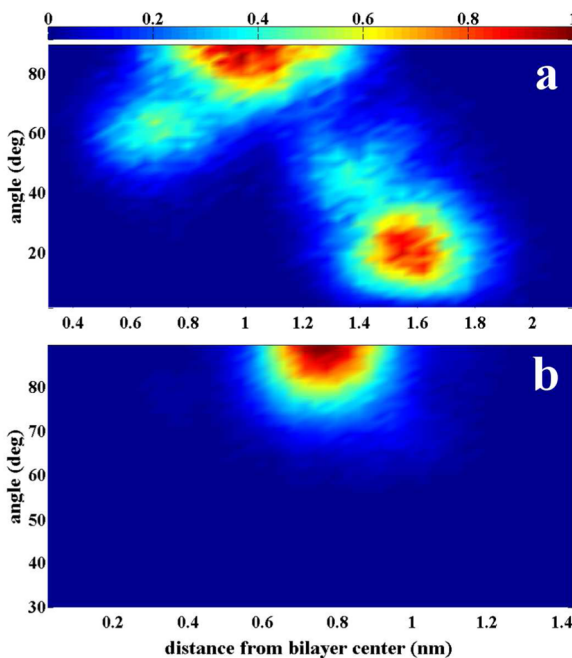


Figure 8. Probability distributions of the angle θ_n between the bilayer normal and the normal of the p-THPP ring plane, shown as a function of the molecule's center of mass position in (a) POPC and (b) DLPC membranes.

For the POPC membrane (Figure 8a), the p-THPP molecules located close to the membrane interface (1.6 nm from membrane center) are arranged so that θ_n has an average value of 20° . Thus, a vector parallel to the plane of the porphyrin ring should make an average angle of 70° with the bilayer normal; the plane of the porphyrin ring aligns almost in parallel to the bilayer surface, as is also highlighted by Figure 2b. At first sight this orientation might look unreasonable as this part of the bilayer is the most ordered and rigid. If a molecule at this position would, however, adopt a parallel orientation to the bilayer normal, its upper part would stick to the water phase. Such a situation would be energetically (entropically) unfavorable; thus, the adopted orientation is more optimal as it reduces the degree of contact between water and the hydrophobic surface of the porphyrin ring. This position and orientation are additionally stabilized by polar interactions as four hydroxyl groups are capable to form hydrogen bonds. The molecules located deeper within the membrane core (1.0 nm from the membrane center) are characterized by an average angle (θ_n) of 90° . This indicates that their ring plane aligns parallel to the bilayer normal. A similar arrangement was found for the porphyrin molecules embedded in the DLPC membrane, as illustrated in Figure 8b.

3.2.2. p-THPP in PEGylated Membranes. Equilibration. Next, we considered the behavior of p-THPP in the presence of the PEGylated bilayer. We performed simulations of three different systems with p-THPP molecules inserted at different positions and with different orientations to the bilayers. Figure 3 depicts snapshots of the initial and final configurations of the simulated systems. The trajectories of the center of mass of porphyrin along the normal to the DLPC/DLPE-PEG membrane during the simulations are shown in Figure S5. For the system M3, all p-THPP molecules, initially placed in the aqueous phase, entered the PEG layer during the first 20 ns of simulations and remained there for the entire simulation

time (Figure SSa). Two molecules formed a dimer in 50 ns (Figure 3b). The other two were in close contact but were separated by PEG chains. This arrangement was maintained for the remainder of the simulation. For this reason, we constructed the system M4, in which a single molecule was placed in the aqueous phase, in order to avoid dimerization and its possible effect on porphyrin location and dynamics. Also in this case the p-THPP molecule remained within the PEG layer. On the other hand, p-THPP molecules initially placed in the hydrocarbon core (systems M4 and M5) remained there for the full course of the simulation. Thus, we did not identify any cases in which the molecules would have translocated between the lipid bilayer and the PEG layer (Figure SS).

Porphyrin Location. Selected snapshots, taken at the end of the simulations and illustrating the location and orientation of porphyrin in the PEGylated bilayer, are shown in Figures 3b, 3d, and 3f. They indicate that p-THPP preferred to lie either inside the membrane core or within the PEG corona. To gain more quantitative information about the location of porphyrin with respect to lipid molecules, we calculated the mass density profiles across the membrane.

Figure 9 shows the average mass density profiles for the lipid phosphate groups, the PEG chains, and the porphyrin rings. For the system M3, the porphyrin profile has only one peak with a maximum at 3.7 nm, which completely overlaps the profile of PEG. For the system M4, two peaks can be observed in the density profile: one at a distance of ~ 0.4 nm

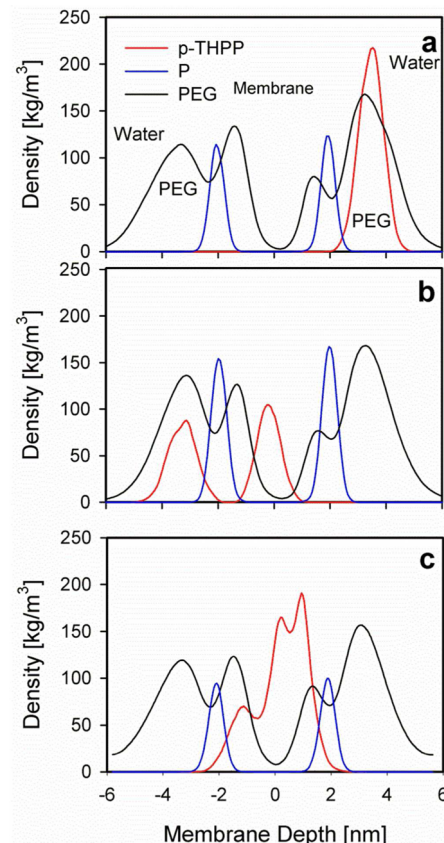


Figure 9. Mass density profiles of porphyrins and selected lipid atoms along the bilayer normal as averaged over the last 100 ns of the trajectories for the systems (a) M3, (b) M4, (c) and M5. The profiles are colored as red (porphyrin rings), blue (phosphate groups), and black lines (PEG chains).

corresponding to porphyrin in the hydrocarbon core and another at a distance of 3.7 nm from the bilayer center, corresponding to p-THPP in the PEG layer. For the system M5, we observed two maxima in the profile, both located in the lipid acyl chain region and centered at distances of ~ 0.4 and ~ 1 nm from the membrane center.

More quantitative information about the location of p-THPP in systems containing PEGylated membranes can be obtained from free energy calculations (system “umbrella DLPE-PEG”). The free energy profile of a p-THPP molecule along the normal of a DLPC/DLPE-PEG bilayer is shown in Figure 10. Two

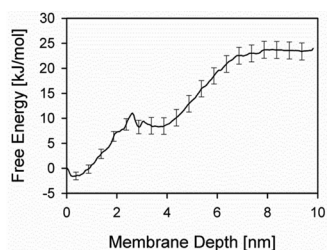


Figure 10. Free energy profile of a p-THPP molecule along the normal of a DLPC/DLPE-PEG bilayer. Depth of zero corresponds to membrane center.

minima at distances of 0.45 and 3.6 nm from the bilayer center are clearly visible. They correspond to p-THPP positions deep inside the bilayer and in the PEG corona, respectively. Moreover, the calculations indicate that the free energy barrier for translocation between the membrane leaflets is substantially lower (1.6 kJ/mol) than that for the non-PEGylated bilayer. Therefore, movement of the solute between membrane leaflets is possible in PEGylated membranes. Figures S5b (blue line) and S5c (green line) show that two of the seven p-THPP molecules that were initially placed inside the DLPC/DLPE-PEG bilayer migrated between the membrane leaflets.

Orientation of Porphyrin in a Membrane. The orientation of p-THPP that is inside PEGylated membranes is shown in Figure 11 as a function of molecule location. The distribution

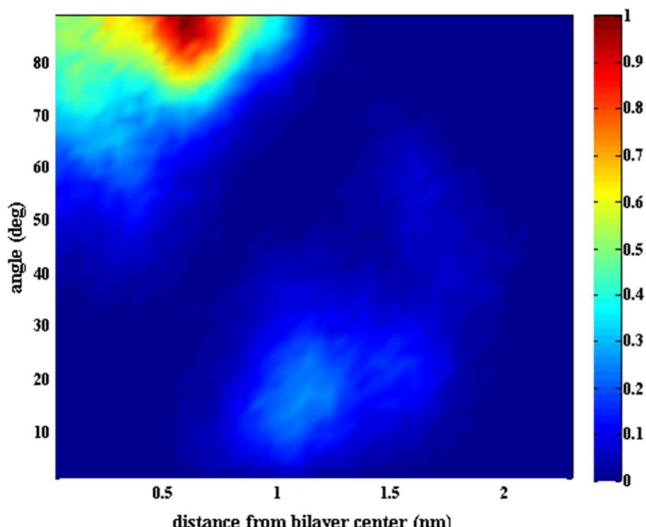


Figure 11. Probability distribution of the angle θ_n between the bilayer normal and the normal to the p-THPP ring, shown as a function of molecule center of mass location in the DLPC/DLPE-PEG membrane.

of p-THPP molecules located deep inside the membrane (~ 0.55 nm) shows that the vector that is normal to the ring plane makes an average angle of 90° with the bilayer normal. Therefore, porphyrin rings align parallel to the bilayer normal. The probability distributions show that the p-THPP molecules can be also located at ~ 1 nm from the membrane center with their ring planes aligned almost parallel to the bilayer surface, characterized by an average θ_n angle of 20° .

4. DISCUSSION

In this study, we considered how the presence of a PEG corona at the surface of lipid membranes affects the behavior of hydrophobic molecules. Especially we clarified the effect of membrane PEGylation on the migration of porphyrin into a membrane and its location therein. The polymer length was chosen to be 45 units, corresponding to a molecular weight of about 2000 Da. This molecular weight has previously been shown to be the most effective in a biological application and is the most commonly used form of PEGylated lipids in pharmaceutical applications.^{43,44} Incorporation of PEGylated lipids to a liposomal membrane can lead to the transformation of vesicular structures into mixed micelles; the effect of the PEG₂₀₀₀-DSPE content on the micelle formation was previously studied.⁴⁵ The micelle formation was observed after incorporation of more than 10 mol % of PEG₂₀₀₀-DSPE. Thus, our experimental studies were performed for systems containing 7 mol % of the PEG-lipid to ensure that only liposomes were present in solution. In the case of the MD simulations, a slightly higher concentration of the PEGylated lipid (9 mol %) was used, since such a membrane was previously constructed and equilibrated.¹⁴

We performed comprehensive atomistic MD simulations of systems containing pure and PEGylated membranes. The simulations were complemented with depth-sensitive fluorescent quenching analyses of porphyrin location in the studied membranes.

There are several experimental pieces of evidence confirming that p-THPP can interact both with conventional and PEGylated lipid bilayers.^{1,46,47} It has been shown that the binding constant of p-THPP to POPC liposomes is equal to 105 ± 35 (mg/mL)⁻¹, indicating that porphyrin has a high affinity for partitioning into lipid membranes. For PEGylated membranes, this value has been found to be dependent on PEG-lipid content: it increased from 237 to 270 (mg/mL)⁻¹ as the concentration of PEG-lipid in a bilayer increased from 3 to 10 mol %. Thus, the presence of the PEG corona at the surface of liposomes improves partitioning of hydrophobic substances to lipid membranes. However, the reasons for this improved partitioning of hydrophobic compounds to SSL liposomes are not clearly understood.

Generally, the arrangement of porphyrins inside a lipid bilayer is relatively poorly understood. In a previous paper, we used MD simulations to study the location, orientation, and dynamics of hematoporphyrin (Hp), a dipropionic porphyrin, inside a POPC bilayer.⁴⁸ It was found that Hp molecules reside preferentially in the lipid carbonyl region of a membrane (about 1.7 nm from the bilayer center). On the other hand, we have also shown that the spatial distribution of p-THPP (a tetraarylporphyrin) in a POPC bilayer is more complex.⁴⁹ It is characterized by two preferred positions: one at 1.51 nm from the bilayer center, corresponding to a location of the lipid carbonyl groups, and another at 0.81 nm from the bilayer center. To gain more detailed insight into the preferred

arrangement of p-THPP in lipid membranes, here we performed simulations in two different bilayers, namely POPC and DLPC. The results of the simulations are in line with experimental findings reported in this paper: p-THPP readily enters both bilayers, confirming its high affinity to a lipophilic environment. However, the simulations revealed that the arrangement of p-THPP embedded in the two studied membranes is different.

In recent studies, phospholipid–porphyrin compounds were synthesized and shown to be useful in drug delivery systems, as the permeability of liposomes composed of these lipids was increased by near-infrared light.⁵⁰ This suggests that these compounds could be used as a trigger for a controlled release of the liposome load. MD simulations showed a similar location of the porphyrin ring to Hp with hydrophilic groups exposed to the membrane interface.

One should be aware of the dimensions of p-THPP and the thickness of lipid bilayers. The optimized structure of porphyrin is shown in Figure S1. The dye molecule is shaped like a square with a side length of 1.3 nm as measured between two oxygen atoms in the hydroxyl groups on the same side of the porphyrin ring. Moreover, the phenyl groups are arranged almost perpendicular to the plane of the porphine ring. Regarding membrane thickness, it is reasonable to consider this parameter as an average N–N spacing (the distance between average positions of choline nitrogen atoms in two leaflets of a lipid bilayer).⁴⁷ We calculated the thickness as 4.2 ± 0.2 and 4.73 ± 0.2 nm for the POPC and DLPC membranes, respectively. Thus, the thicknesses of one leaflet of the POPC and DLPC membranes are about 2.1 and 2.36 nm, respectively, confirming that p-THPP is relatively large compared to dimensions of the lipid bilayers.

In DLPC bilayers, all porphyrin molecules were localized at the same depth in the bilayer (about 0.8 nm from the membrane center) and adopted a similar alignment with respect to lipids, as shown in Figures 6b and 8b. The orientation of p-THPP inside a membrane should be analyzed in comparison to the orientation of the lipid acyl chains. The average tilt angle of the linoleoyl chains was calculated from the cosine of the angle between the bilayer normal and the average vector linking the carbon atom at the end of the linoleoyl chain and the carbonyl carbon atom of the same chain. By doing so, the average tilt angle of the acyl chains in the DLPC bilayer was found to be $\sim 25^\circ$. Since the porphyrin plane is parallel to the bilayer normal, it makes an angle of about 25° with the lipid molecules. For the POPC membrane, the shape of the density profile of p-THPP indicates two preferential locations within the POPC membrane: one closer to the water–membrane interface and the second one deeper within the membrane, at distances of 1.5 and 0.8 nm from the membrane center, respectively. The orientation of the dye molecules is different in these two positions. The p-THPP molecules immersed deeply in the POPC membrane adopted an orientation where their plane was perpendicular to the membrane surface. The average tilt angle for the palmitoyl groups was calculated to be $\sim 31^\circ$. Thus, the ring plane made an angle of about 30° with the lipid acyl chains. On the other hand, the dye molecules located in the interface between the hydrocarbon chain region and the polar region were almost parallel to the membrane surface.

The differences in arrangements of p-THPP in the two bilayers can be explained given their different properties. Porphyrin contains four electronegative oxygen atoms symmetrically distributed in the corners of the porphyrin ring.

These atoms bear relatively high partial charges of -0.53 . These charges on the hydroxyl oxygens would enforce them to be excluded from the membrane hydrocarbon core and to interact with the polar headgroups of a membrane. Both lipids have the same headgroup, but differ in area per molecule. This area parameter is 0.651 ± 0.004 and 0.633 ± 0.002 nm² for POPC and DLPC membranes, respectively. Thus, the DLPC bilayer is more densely packed and thicker compared to the POPC bilayer, indicating that the ordering of acyl chains is higher for DLPC. Therefore, the p-THPP molecules are forced to adopt the orientation of the lipid hydrocarbon chains with only two hydroxyl groups directed to the polar region of the DLPC membrane. Meanwhile, POPC has in its structure two different acyl chains (Figure S2). The bending of oleoyl chains by 30° at the C9 position causes a reduction of acyl chain ordering in the bilayer, increasing membrane free volume (the unoccupied volume enclosed within the bilayer¹). Thus, the lipid molecules are moved apart, as indicated by the value of the area per molecule. As a result, p-THPP molecules have some freedom of orientation and a fraction of them can be arranged almost parallel to the membrane surface with all four hydroxyl groups situated close to the headgroups of the bilayer.

Figure 9 shows that the mass density profiles of PEG have two maxima: one in the outside of a bilayer (at ~ 3.7 nm from the membrane center) and another inside a lipid membrane (about 1.4 nm from the membrane center). This indicates that some of the PEG chains can penetrate into the membrane interior. These results are in agreement with our previous simulations¹⁴ showing that a portion of the PEG layer penetrates the lipid core of the membrane. The presence of the polymer changes membrane properties; in comparison to a neat membrane, the area per lipid for the DLPC/DLPE-PEG system is increased to 0.7 ± 0.003 nm², while the thickness of the membrane is decreased to 4.25 ± 0.02 nm. This indicates that PEGylated membranes are more expanded, and their free volume is increased. The increase in free volume of a membrane in the liquid state upon PEGylation has been previously shown experimentally, but until now its molecular interpretation has been, however, unknown.¹

The change of membrane properties upon PEGylation has an effect on porphyrin arrangement within the DLPC/DLPE-PEG bilayer. Our MD simulations clearly show that the incorporation of a PEGylated lipid into a membrane lipid composition has a significant impact on porphyrin location. There are two preferred positions: deep inside a membrane (the porphyrin center of mass at the distance of 0.4 nm from the membrane center) and in the PEG layer (at ca. 3.7 nm from the membrane center). The penetration of the polymer into the DLPC membrane is the reason why the minimum of the free energy profile calculated for p-THPP molecules shifted about 0.4 nm toward the center of the membrane (Figure 10). However, the orientation of porphyrin molecules was not changed. The ring planes of p-THPP are perpendicular to the membrane surface.

The presence of porphyrin in the PEG corona can be explained through the properties of the polymer. It has been shown that a hydrophobic molecule can interact with PEG, since this polymer is not completely hydrophilic.^{32,48} This interaction is lipophilic in nature; the nonpolar (CH₂)₂ groups of a PEG chain interact with the nonpolar surface of the molecule.³² p-THPP is a highly hydrophobic molecule as indicated by the lipophilicity parameter: log P equals 6.88.⁴⁸ Thus, it is expected that the interaction between porphyrin and PEG is strong. The hydrophobic ethylene groups of PEG

chains adhere strongly to the hydrophobic porphyrin ring. As a result, porphyrin molecules are densely wrapped with the PEG chains; we have observed a similar result concerning hydrophobic targeting ligands in a previous study.⁵¹ The strong interaction between PEG and porphyrin is particularly noteworthy from the perspective of the PEGylation of drug delivery liposomes. If there is a strong interaction between the PEG layer and drug molecules being carried by a PEGylated liposome, then this may form an extra barrier against release. Additionally, it is possible that some drug molecules are being carried in the PEG layer rather than in the water cavity within the liposome.

An interesting result found from the simulations is that porphyrin can form dimers in the PEG layer. The aggregation phenomenon of p-THPP in an aqueous environment has previously been studied, and the dimerization equilibrium constant, K_D , was found to be $1.2 \times 10^5 \text{ M}^{-1}$.⁴⁶ Thus, porphyrin molecules in aqueous solutions are present mostly in the aggregated form. Since both p-THPP dimerization and the interactions between PEG and p-THPP are driven by contact with the hydrophobic surfaces of porphyrin, it can be assumed that these interactions compete. Thus, increased interaction with PEG is expected to result in decreasing dimerization. In our previous studies we showed that increasing PEG concentration causes the aggregation of hemotoporphyrin to decrease.³²

The FQA experiments were performed to validate the results of the computer simulations. For POPC membranes, the efficiency of quenching by copper cations is low. This means that p-THPP is located inside a membrane and thereby protected from contact with the quencher. In the next step, quenching experiments were performed using lipids with a quenching moiety attached to different vertical positions at pH 9. The effect of pH on the partitioning of p-THPP into liposomes is negligible under our experimental conditions (Figure S3 in the Supporting Information). These measurements showed that the most effective quenching process was achieved when the quenching groups were located at the interface between polar and hydrophobic membrane regions. This is consistent with the results of MD simulations on the depth of porphyrin in conventional membranes. FQA is not so sensitive to show the differences in the p-THPP location within the POPC and DLPC membranes; therefore, the experiments were performed only for the POPC liposomes.

The quenching process of porphyrin dispersed in PEGylated liposomes by copper dications was 14 times more effective compared to systems containing conventional liposomes. Thus, at least part of the p-THPP molecules was well accessible to the quencher. It has previously been shown that Cu²⁺ ions can form complexes with ethylene oxide units of PEG chains.⁵² Therefore, it is reasonable to assume that the dye molecules are also located in the PEG corona surrounding the lipid surface and remain in close contact with the quenching agents. However, the Stern–Volmer plot was curved downward, indicating unequivocally that a portion of the porphyrin molecules was prevented from making contact with the quencher, as a result of their migration to a membrane. To confirm the presence of porphyrin molecules inside a lipid membrane, the FQA experiments with nitroxide-labeled lipids were carried out. The largest quenching effect was obtained for the molecules with the nitroxide groups situated deep within the membrane core and at the interface of the bilayer–water phases. The latter can be assigned to the quenching of

porphyrin molecules embedded into the PEG layer. Overall, the quenching experiments revealed that p-THPP molecules were located in the PEGylated membrane in two positions: in the PEG layer (accessible for the copper cations) and deep inside the bilayer. Consequently, the experimental findings strongly supported the atomistic MD simulation results.

5. CONCLUSIONS

We used comprehensive computer simulations and fluorescence experiments to investigate the behavior of p-THPP, used as a model for hydrophobic drugs, in the presence of zwitterionic and PEGylated membranes. In agreement with experiments, we found that p-THPP can enter both types of lipid bilayers. Our studies, however, showed also important differences in the behavior of p-THPP embedded in PEGylated membranes. We observed that p-THPP has a greater exposure to the water solvent in comparison to conventional liposomes. We found evidence that p-THPP molecules have two preferred locations in SSL liposomes: deep within the hydrophobic core of a membrane and within the PEG layer surrounding liposomes. Therefore, the main reason for the higher affinity of porphyrin to PEGylated membranes is associated with the appearance of the PEG corona around lipid vesicles. Porphyrin molecules are wrapped by PEG chains attached to lipid molecules. As a result, additional volume for accumulation of hydrophobic molecules is present in sterically stabilized liposomes. Additionally, the incorporation of PEGylated lipids into lipid membranes increases their free volume. Therefore, the loading efficiency of the hydrocarbon region is also improved.

■ ASSOCIATED CONTENT

S Supporting Information

Partial charge calculations; chemical structures of p-THPP and lipids used in this study; trajectories of the center of mass of p-THPP along the bilayer normal for DLPC and POPC; trajectories of the center of mass of p-THPP-PEG in systems containing the PEGylated membrane. The Supporting Information is available free of charge on the ACS Publications website at DOI: 10.1021/acs.jpcb.5b01351.

■ AUTHOR INFORMATION

Corresponding Authors

*Tel +48 12 6632020; Fax +48 12 6340515; e-mail kepczyns@chemia.uj.edu.pl (M.K.).

*Tel +358 40 198 1010; Fax +358 3 3115 3015; e-mail tomasz.rog@gmail.com (T.R.).

Notes

The authors declare no competing financial interest.

■ ACKNOWLEDGMENTS

This project was supported by the National Science Centre Poland on the basis of the decision number DEC-2012/07/B/ST5/00913. T.R. and I.V. thank the Academy of Finland for financial support (Center of Excellence in Biomembrane Research), and I.V. thanks the European Research Council (Advanced Grant project CROWDED-PRO-LIPIDS). For computational resources, we thank CSC-IT Center for Science (Espoo, Finland).

REFERENCES

- (1) Kepczynski, M.; Nawalany, K.; Kumorek, M.; Kobierska, A.; Jachimska, B.; Nowakowska, M. Which Physical and Structural Factors of Liposome Carriers Control Their Drug-Loading Efficiency? *Chem. Phys. Lipids* **2008**, *155*, 7–15.
- (2) Lasic, D. D. Novel Applications of Liposomes. *Trends Biotechnol.* **1998**, *16*, 307–321.
- (3) van Balen, G. P.; Martinet, C. M.; Caron, G.; Bouchard, G.; Reist, M.; Carrupt, P.-A.; Fruttero, R.; Gasco, A.; Testa, B. Liposome/Water Lipophilicity: Methods, Information Content, and Pharmaceutical Applications. *Med. Res. Rev.* **2004**, *24*, 299–324.
- (4) Kępczyński, M.; Pandian, R. P.; Smith, K. M.; Ehrenberg, B. Do Liposome-Binding Constants of Porphyrins Correlate with their Measured and Predicted Partitioning between Octanol and Water? *Photochem. Photobiol.* **2002**, *76*, 127–134.
- (5) Yan, X.; Scherphof, G. L.; Kamps, J. A. Liposome Opsonization. *J. Liposome Res.* **2005**, *15*, 109–139.
- (6) Moghimi, S. M.; Szelenyi, J. Stealth Liposomes and Long Circulating Nanoparticles: Critical Issues in Pharmacokinetics, Opsonization and Protein-Binding Properties. *Prog. Lipid Res.* **2003**, *42*, 463–478.
- (7) Romberg, B.; Oussoren, C.; Snel, C. J.; Carstens, M. G.; Hennink, W. E.; Storm, G. Pharmacokinetics of Poly(hydroxyethyl-l-asparagine)-Coated Liposomes is Superior over that of PEG-Coated Liposomes at Low Lipid Dose and upon Repeated Administration. *Biochim. Biophys. Acta, Biomembr.* **2007**, *1768*, 737–743.
- (8) Torchilin, V. P. Recent Advances with Liposomes as Pharmaceutical Carriers. *Nat. Rev. Drug. Discovery* **2005**, *4*, 145–160.
- (9) Gabizon, A.; Catane, R.; Uziely, B.; Kaufman, B.; Safra, T.; Cohen, R.; Martin, F.; Huang, A.; Barenholz, Y. Prolonged Circulation Time and Enhanced Accumulation in Malignant Exudates of Doxorubicin Encapsulated in Polyethylene-Glycol Coated Liposomes. *Cancer Res.* **1994**, *54*, 987–992.
- (10) Dinc, C. O.; Kibarer, G.; Guner, A. Solubility Profiles of Poly(Ethylene Glycol)/Solvent Systems. II. Comparison of Thermodynamic Parameters from Viscosity Measurements. *J. Appl. Polym. Sci.* **2010**, *117*, 1100–1119.
- (11) Friman, S.; Egestad, B.; Sjovall, J. Hepatic Excretion and Metabolism of Polyethylene Glycols and Mannitol in the Cat. *J. J. Hepatol.* **1993**, *17*, 48–55.
- (12) Yoshida, A.; Hashizaki, K.; Yamauchi, H.; Sakai, H.; Yokoyama, S.; Abe, M. Effect of Lipid with Covalently Attached Poly(Ethylene Glycol) on the Surface Properties of Liposomal Bilayer Membranes. *Langmuir* **1999**, *15*, 2333–2337.
- (13) Tirosh, O.; Barenholz, Y.; Katzhendler, J.; Priev, A. Hydration of Polyethylene Glycol-Grafted Liposomes. *Biophys. J.* **1998**, *74*, 1371–1379.
- (14) Stepniewski, M.; Pasenkiewicz-Gierula, M.; Róg, T.; Danne, R.; Orlowski, A.; Karttunen, M.; Urtti, A.; Yliperttula, M.; Vuorimaa, E.; Bunker, A. Study of PEGylated Lipid Layers as a Model for PEGylated Liposome Surfaces: Molecular Dynamics Simulation and Langmuir Monolayer Studies. *Langmuir* **2011**, *27*, 7788–7798.
- (15) Magarkar, A.; Karakas, E.; Stepniewski, M.; Róg, T.; Bunker, A. Molecular Dynamics Simulation of PEGylated Bilayer Interacting with Salt Ions: A Model of the Liposome Surface in the Bloodstream. *J. Phys. Chem. B* **2012**, *116*, 4212–4219.
- (16) Magarkar, A.; Rög, T.; Bunker, A. Molecular Dynamics Simulation of PEGylated Membranes with Cholesterol: Building toward the DOXIL Formulation. *J. Phys. Chem. C* **2014**, *118*, 15541–15549.
- (17) MacCallum, J. L.; Tielemans, D. P. Interactions between Small Molecules and Lipid Bilayers. *Curr. Top. Membr. Transp.* **2008**, *60*, 227–256.
- (18) Rög, T.; Vattulainen, I. Cholesterol, Sphingolipids, and Glycolipids: What Do We Know about Their Role in Raft-Like Membranes. *Chem. Phys. Lipids* **2014**, *184*, 82–104.
- (19) Bemporad, D.; Luttmann, C.; Essex, J. W. Computer Simulation of Small Molecule Permeation across a Lipid Bilayer: Dependence on Bilayer Properties and Solute Volume, Size, and Cross-Sectional Area. *Biophys. J.* **2004**, *87*, 1–13.
- (20) Kepczynski, M.; Kumorek, M.; Stepniewski, M.; Rög, T.; Kozik, B.; Jamróz, D.; Bednar, J.; Nowakowska, M. Behavior of 2,6-Bis(decyloxy)naphthalene Inside Lipid Bilayer. *J. Phys. Chem. B* **2010**, *114*, 15483–15494.
- (21) Stimson, L.; Dong, L.; Karttunen, M.; Wisniewska, A.; Dutka, M.; Rög, T. Stearic Acid Spin Labels in Lipid Bilayers: Insight through Atomistic Simulations. *J. Phys. Chem. B* **2007**, *111*, 12447–12453.
- (22) Gabizon, A.; Catane, R.; Uziely, B.; Kaufman, B.; Safra, T.; Cohen, R.; Martin, F.; Huang, A.; Barenholz, Y. Prolonged Circulation Time and Enhanced Accumulation in Malignant Exudates of Doxorubicin Encapsulated in Polyethylene-Glycol Coated Liposomes. *Cancer Res.* **1994**, *54*, 987–992.
- (23) Magarkar, A.; Rög, T.; Bunker, A. Molecular Dynamics Simulation of Pegylated Membranes with Cholesterol: Building towards the DOXIL Formulation. *J. Phys. Chem. C* **2014**, *118*, 5541–5549.
- (24) Kästner, J. Umbrella Sampling. *Wiley Interdiscip. Rev.: Comput. Mol. Sci.* **2011**, *1*, 932–942.
- (25) Hub, J. S.; de Groot, B. L.; van der Spoel, D. g_wham — A Free Weighted Histogram Analysis Implementation Including Robust Error and Autocorrelation Estimates. *J. Chem. Theory Comput.* **2010**, *6*, 3713–3720.
- (26) Nandy, B.; Maiti, P. K.; Bunker, A. Force Biased Molecular Dynamics Simulation Study of Effect of Dendrimer Generation on Interaction with DNA. *J. Chem. Theory Comput.* **2013**, *9*, 722–729.
- (27) St-Pierre, J.-F.; Karttunen, M.; Mousseau, N.; Rög, T.; Bunker, A. Use of Umbrella Sampling to Calculate the Entrance/Exit Pathway for Z-Pro-Proline Inhibitor in Prolyl Oligopeptidase. *J. Chem. Theory Comput.* **2011**, *7*, 1583–1594.
- (28) Filipe, H. A. L.; Moreno, M. J.; Rög, T.; Vattulainen, I.; Loura, L. M. S. How to Tackle the Issues in Free Energy Simulations of Long Amphiphiles Interacting with Lipid Membranes: Convergence and Local Membrane Deformations. *J. Phys. Chem. B* **2014**, *118*, 3572–3581.
- (29) Hess, B.; Kutzner, C.; van der Spoel, D.; Lindahl, E. GROMACS 4: Algorithms for Highly Efficient, Load-Balanced, and Scalable Molecular Simulation. *J. Chem. Theory Comput.* **2008**, *4*, 435–447.
- (30) Jorgensen, W. L.; Maxwell, D. S.; Tirado-Rives, J. Development and Testing of the OPLS All-Atom Force Field on Conformational Energetics and Properties of Organic Liquids. *J. Am. Chem. Soc.* **1996**, *118*, 11225–11236.
- (31) Maciejewski, A.; Pasenkiewicz-Gierula, M.; Cramariuc, O.; Vattulainen, I.; Rög, T. Refined OPLS-AA Force Field for Saturated Phosphatidylcholine Bilayers at Full Hydration. *J. Phys. Chem. B* **2014**, *118*, 4571–4581.
- (32) Li, Y.-C.; Rissanen, S.; Stepniewski, M.; Cramariuc, O.; Rög, T.; Mirza, S.; Xhaard, H.; Wytrwal, M.; Kepczynski, M.; Bunker, A. Study of Interaction between PEG Carrier and 3 Relevant Drug Molecules: Piroxicam, Paclitaxel, and Hematoporphyrin. *J. Phys. Chem. B* **2012**, *116*, 7334–7341.
- (33) Jorgensen, W. L.; Chandrasekhar, J.; Madura, J. D.; Impey, R. W.; Klein, M. L. Comparison of Simple Potential Functions for Simulating Liquid Water. *J. Chem. Phys.* **1983**, *79*, 926–935.
- (34) Bussi, G.; Donadio, D.; Parrinello, M. Canonical Sampling through Velocity Rescaling. *J. Chem. Phys.* **2007**, *126*, 1–7.
- (35) Parrinello, M.; Rahman, A. Polymorphic Transitions in Single Crystals: A New Molecular Dynamics Method. *J. Appl. Phys.* **1981**, *52*, 7182–7190.
- (36) Darden, T.; York, D.; Pedersen, L. Particle Mesh Ewald: An Nlog(N) Method for Ewald Sums in Large Systems. *J. Chem. Phys.* **1993**, *98*, 10089–10092.
- (37) Hess, B.; Bekker, H.; Berendsen, H. J. C.; Fraaije, J. G. E. M. LINCS: A Linear Constraint Solver for Molecular Simulations. *J. Comput. Chem.* **1997**, *18*, 1463–1472.
- (38) Rog, T.; Pasenkiewicz-Gierula, M. Cholesterol Effects on a Mixed-Chain Phosphatidylcholine Bilayer: a Molecular Dynamics Simulation Study. *Biochimie* **2006**, *88*, 449–460.

- (39) Chattopadhyay, A.; London, E. Parallax Method for Direct Measurement of Membrane Penetration Depth Utilizing Fluorescence Quenching by Spin-Labeled Phospholipids. *Biochemistry* **1987**, *26*, 39–45.
- (40) Dwiecki, K.; Górnáś, P.; Wilk, A.; Nogala-Kalucka, M.; Polewski, K. Spectroscopic Studies of D-alpha-Tocopherol Concentration-Induced Transformation in Egg Phosphatidylcholine Vesicles. *Cell. Mol. Biol. Lett.* **2007**, *12*, 51–69.
- (41) Lakowicz, J. R. *Principles of Fluorescence Spectroscopy*; Plenum Press: New York, 1983.
- (42) Binder, H.; Zschörnig, O. The Effect of Metal Cations on the Phase Behavior and Hydration Characteristics of Phospholipid Membranes. *Chem. Phys. Lipids* **2002**, *115*, 39–61.
- (43) Maruyama, K.; Yuda, T.; Okamoto, A.; Ishikura, C.; Kojima, S.; Iwatsuru, M. Effect of Molecular Weight in Amphiphatic Polyethyleneglycol on Prolonging the Circulation Time of Large Unilamellar Liposomes. *Chem. Pharm. Bull.* **1991**, *39*, 1620–1622.
- (44) Mori, A.; Klibanov, A. L.; Torchilin, V. P.; Huang, L. Influence of the Steric Barrier Activity of Amphiphatic Poly(Ethyleneglycol) and Ganglioside GM1 on the Circulation Time of Liposomes and on the Target Binding of Immunoliposomes in Vivo. *FEBS Lett.* **1991**, *284*, 263.
- (45) Ueno, M.; Sriwongsitanont, S. Effect of PEG Lipid on Fusion and Fission of Phospholipid Vesicles in the Process of Freeze-Thawing. *Polymer* **2005**, *46*, 1257–1267.
- (46) Nawalany, K.; Rusin, A.; Kepczynski, M.; Mikhailov, A.; Kramer-Marek, G.; Snieta, M.; Poltowicz, J.; Krawczyk, Z.; Nowakowska, M. Comparison of Photodynamic Efficacy of Tetraarylporphyrin Pegylated or Encapsulated in Liposomes: In Vitro Studies. *J. Photochem. Photobiol., B* **2009**, *97*, 8–17.
- (47) Nawalany, K.; Kozik, B.; Kepczynski, M.; Zapotoczny, S.; Kumorek, M.; Nowakowska, M.; Jachimska, B. Properties of Polyethylene Glycol Supported Tetraarylporphyrin in Aqueous Solution and Its Interaction with Liposomal Membranes. *J. Phys. Chem. B* **2008**, *112*, 12231–12239.
- (48) Stępniewski, M.; Kepczynski, M.; Jamróz, D.; Nowakowska, M.; Rissanen, S.; Vattulainen, I.; Róg, T. Interaction of Hematoporphyrin with Lipid Membranes. *J. Phys. Chem. B* **2012**, *116*, 4889–4897.
- (49) Rissanen, S.; Kumorek, M.; Martinez-Seara, H.; Li, Y.-C.; Jamroz, D.; Bunker, A.; Nowakowska, M.; Vattulainen, I.; Kepczynski, M.; Rog, T. Effect of PEGylation on Drug Entry into Lipid Bilayer. *J. Phys. Chem. B* **2014**, *118*, 144–151.
- (50) Carter, K. A.; Shao, S.; Hoopes, M. I.; Luo, D.; Ahsan, B.; Grigoryants, V. M.; Song, W.; Huang, H.; Zhang, G.; Pandey, R. K.; Geng, J.; Pfeifer, B. A.; Scholes, C. P.; Ortega, J.; Karttunen, M.; Lovell, J. F. Porphyrin–Phospholipid Liposomes Permeabilized by Near-Infrared Light. *Nat. Commun.* **2014**, *5* (3546), 1–11.
- (51) Lehtinen, J.; Magarkar, A.; Stepniewski, M.; Hakola, S.; Bergman, M.; Rog, T.; Yliperttula, M.; Urtti, A.; Bunker, A. Evidence from Molecular Modeling that Coverage by PEG-Sheath is Cause of Hampered Targeting Results for Liposomes Conjugated with Hydrophobic Peptide. *Eur. J. Pharm. Sci.* **2012**, *46*, 121–130.
- (52) Stoychev, D.; Tsvetanov, C. Behaviour of Poly(ethylene glycol) during Electrodeposition of Bright Copper Coatings in Sulfuric Acid Electrolytes. *J. Appl. Electrochem.* **1996**, *26*, 741–749.